Published in final edited form as:
J Neurosci Methods. 2015 February 15; 241: 132–136. doi:10.1016/j.jneumeth.2014.12.017.

Spatial characterization of a multifunctional pipette for drug delivery in hippocampal brain slices

Aikeremu Ahemaiti[a], **Holger Wigström**[b], **Alar Ainla**[a], **Gavin D.M. Jeffries**[a], **Owe Orwar**[a], **Aldo Jesorka**[a], and **Kent Jardemark**[c,*]

[a]Department of Chemical and Biological Engineering, Chalmers University of Technology, Kemivägen 10, SE-41296 Göteborg, Sweden

[b]Institute of Neuroscience and Physiology, The Sahlgrenska Academy at Göteborg University, Box 430, SE-405 30 Göteborg, Sweden

[c]Department of Physiology and Pharmacology, Karolinska Institutet, SE-17177, Stockholm, Sweden

Abstract

Background—Among the various fluidic control technologies, microfluidic devices are becoming powerful tools for pharmacological studies using brain slices, since these devices overcome traditional limitations of conventional submerged slice chambers, leading to better spatiotemporal control over delivery of drugs to specific regions in the slices. However, microfluidic devices are not yet fully optimized for such studies.

New Method—We have recently developed a multifunctional pipette (MFP), a free standing hydrodynamically confined microfluidic device, which provides improved spatiotemporal control over drug delivery to biological tissues.

Results—We demonstrate herein the ability of the MFP to selectively perfuse one dendritic layer in the CA1 region of hippocampus with CNQX, an AMPA receptor antagonist, while not affecting the other layers in this region. Our experiments also illustrate the essential role of hydrodynamic confinement in sharpening the spatial selectivity in brain slice experiments. Concentration-response measurements revealed that the ability of the MFP to control local drug concentration is comparable with that of whole slice perfusion, while in comparison the required amounts of active compounds can be reduced by several orders of magnitude.

Comparison with Existing Method—The multifunctional pipette is applied with an angle, which, compared to other hydrodynamically confined microfluidic devices, provides more accessible space for other probing and imaging techniques.

*Corresponding author at: Department of Physiology and Pharmacology, Karolinska Institutet, SE-17177, Stockholm, Sweden. Tel.: +46-8-52487918; Fax: +46-8-308424, Kent.Jardemark@ki.se.

Conflict of interest: None of the authors have any conflicts of interest to disclose.

Conclusions—Using the MFP it will be possible to study selected regions of brain slices, integrated with various imaging and probing techniques, without affecting the other parts of the slices.

Introduction

Pharmacological tests on single cells or groups of cells in living tissue, such as brain slices and tissue cultures, generally require precise control of the chemical environment. Well-controlled chemical stimulation protocols, above all the determination of concentration-response curves, are typically required in pharmacological studies on cellular networks *in situ*, where they significantly contribute to increase the understanding of complex mechanisms of action of drugs and other bioactive compounds. The currently available tools are, however, limited in their temporal and spatial specificity, not to mention that they often do not minimize the amount of drug used. To date, there are a number of micro-perfusion tools, *e.g.*, glass micropipettes (Ling and Gerard, 1949, Neher and Sakmann, 1976, Huang et al., 2012), and microfluidic perfusion chambers (Blake et al., 2007), for delivery of chemical stimulus to the vicinity of cells in tissue slices or cultures, allowing substantial savings of expensive drugs. However, these devices are not optimal in the sense that they are unable to maintain a localized perfusion without causing diffusion of the bioactive compound from the target region, e.g. a cell layer or an isolated cell (Huang et al., 2012), to nearby areas that may or may not be part of the cellular network being studied.

The optimal device for perfusion of cells in tissues or cultures should allow for contamination-free, repetitive administrations of different concentrations of the bioactive compound without the need of exchanging or even moving the delivery device, such as a pipette needle, while addressing a specific individual cell or group of cells in a biological preparation. In order to accomplish these requirements, we have developed a free-standing microfluidic device, the multifunctional pipette (MFP) in polydimethylsiloxane (Ainla et al., 2010, Ainla et al., 2012a). This pipette utilizes an advanced fluid recirculation principle which provides a hydrodynamically confined flow (HCF), *i.e.*, a closely confined virtual flow cell that enables high-resolution spatial control of the distribution of a biological active substance(s) administered to a specific cell layer or an isolated cell. Previously, we have shown applications of this MFP in different experimental setups. Using, for example, an uptake assay, we have shown that the MFP can be used to generate concentration-response curves *in situ* of proton-activated human transient receptor potential vanilloid (*h*TRPV1) receptors expressed in cultured and adherent Chinese hamster ovary cells (Ainla et al., 2010). Moreover, practical use of the MFP in conjunction with electrophysiological recordings of these cells by the patch clamp technique was also demonstrated (Ainla et al., 2010). Recently, we have examined the compatibility of the multifunctional pipette with electrophysiological recordings of pyramidal cells in hippocampal and prefrontal cortex brain slices from rats (Ahemaiti et al., 2013). In that work, we determined the dependence of the responses of these recordings on the distance of the MFP from the recording site, documented a multifold gain in solution exchange time as compared to whole slice perfusion, and showed that the device is able to store and deliver up to four solutions in a series (Ahemaiti et al., 2013). Thus, we have demonstrated the use of the MFP for localized

perfusion of bioactive compounds, showing that the microfluidic device is compatible with other probing devices, such as electrophysiological recording equipment.

Here, we continue and extend the characterization of the MFP in conjunction with electrophysiological extracellular recordings of cells in rat hippocampal brain slices. Special emphasis is put on spatial specificity as determined from the drug effect on hippocampal electric activity and its dependence on distance between the site of activity and the MFP. The hippocampal formation plays an important role in establishing episodic and declarative memories (Tulving and Markowitsch, 1998, Eichenbaum, 1999, Rolls, 2010, Travis et al., 2014). With reference to its importance in normal functions as well as in several diseases (e.g. schizophrenia and depression) (Stockmeier et al., 2004, Tanti and Belzung, 2013), the hippocampal brain slice has been intensely used as a model for studying e.g. long-term potentiation, a mechanism underlying the generation of certain memories (see above), and for studies of mechanism of drugs actions in hippocampus-related diseases. We demonstrate herein the spatial capabilities of the MFP to specifically administer the amino-3-hydroxy-5-methyl-4-isoxazolepropionic acid (AMPA) receptor antagonist 6-cyano-7-nitroquinoxaline-2,3-dione (CNQX) to electrophysiologically recorded pyramidal cells within different layers in the CA1 region of hippocampus.

Materials and Methods

Hippocampus slice preparation

Sprague-Dawley rats (2- to 8-week old, Charles River, Germany) were used for preparing the hippocampus slices. The procedures were conducted following the guidelines of the Swedish Council for Laboratory Animals and were approved by the Gothenburg Ethical Committee for Animal Experimentation. The rats were anesthetized with isoflurane (Isoba®Vet) and the hippocampi were isolated immediately after decapitation. Hippocampi were then cut transversely into 400 μm thick slices by an in-home designed McIlwain-type tissue chopper and placed in a holding chamber with continuously oxygenated (95% O_2 /5% CO_2) Ringer's solution (NaCl 120 mM; KCl 2.5 mM; NaH_2PO_4 1 mM; $NaHCO_3$ 26 mM, $CaCl_2$ 2 mM, $MgCl_2$ 6 mM) at room temperature for recovery. After at least 90 min of recovery, the slices were transferred into a recording chamber where they were fixed by a net in a continuously superfusing solution saturated with 95% O_2 and 5% CO_2, at 30°C. The perfusion solution was similar to the Ringer's solution used in preparation of the slices, except that 2 mM $MgCl_2$ instead of 6 mM was used. Experiments were conducted after 15-30 min adaptation of the slices in the perfusion chamber.

Extracellular recording of field excitatory postsynaptic potentials (fEPSPs) in the hippocampus

Tungsten microelectrodes (type TM33B01, World precision Instruments, Inc.) were used to stimulate the Schaffer collateral pathway in the CA1 region. Negative constant-current pulses (-20 to -60 μA) with a duration of 100 μs were delivered via a stimulating microelectrode by an in-house developed adjustable pulse generator at a rate of 0.1-0.2 Hz. Extracellular field potentials were recorded in the middle of the pyramidal cell apical dendritic layer (stratum radiatum), 200-500 μm away from the stimulating electrode and at a

depth of 100-150 μm below the surface of the slice, using a glass pipette filled with 1 mM NaCl (resistance 2-4 MΩ; made from borosilicate glass capillaries GC150F-10, Harvard apparatus, UK; pulled by a PP-83, Narishige Scientific Instrument Lab, Japan). The signals were amplified, filtered, digitized (16 bit multi-channel A/D interface board) and transferred to an IBM-PC/AT compatible computer for monitoring and analysis, by Eagle Technology (RSA) based in-house designed electronic equipment, and software written in QuickBASIC (Microsoft Corporation).

Offline data analysis was conducted by means of the pCLAMP-Clampfit software (Molecular Devices, CA, USA). The slope of the recorded early fEPSP, which was mediated dominantly by AMPA-type glutamate receptors, was measured. This measurement represents the efficacy of AMPA receptor-mediated synaptic transmission (Muller *et al.*, 1988, 1989; Shahi and Baudry, 1992).

Drugs and buffer

KCl, NaH_2PO_4, $CaCl_2$ and $NaHCO_3$ were all obtained from Merck (Darmstadt, Germany). $MgCl_2$ and glucose were purchased from VWR international (Leicestershire, UK), NaCl from Riedel deHaen (Seelze, Germany). The competitive AMPA/kainate receptor antagonist 6-cyano-7-nitroquinoxaline-2,3-dione (CNQX) was obtained from Tocris Bioscience (Bristol, UK) or Ascent Scientific Ltd. (UK). Isoflurane (Isoba®Vet) was obtained from MSD animal health (Bergen, Norway).

Multifunctional pipette (MFP)

The operation parameters of the MFP, such as the range of supply pressure and vacuum, as well as the inflow/outflow ratio, which determine the properties of the HCF, were selected according to the previous description of the MFP (Ainla et al., 2012a, Ainla et al., 2012b, Ahemaiti et al., 2013). Solutions were filtered through a 0.2 μm syringe filter (Acrodisc® CR 13 mm Syringe Filter, PALL life science, USA) before loading the pipette for preventing blockage within the pipette channels. The distance from the pipette tip to the tissue surface was kept at ∼10 μm during the experiment, while the pipette was horizontally moved and selectively applied to different parts of the tissue, *i.e.*, the desired layers in the CA1 region of the hippocampus. The drug delivery performance of the MFP was measured by means of concentration response curves of CNQX in comparison with bath perfusion. The latter is the most commonly used method in tissue slice studies, where tissue is soaked in the circulated drug solution in the bath. The spatial drug delivery profile of the MFP was determined with and without HCF by turning the aspiration on and off, respectively.

Data processing

MS Excel, Matlab, and Graphpad Prism were used for various parts of the data analysis and curve fitting. Comsol Multiphysics software was employed for modeling of diffusion in the brain slice, using the “transport of diluted species” feature.

Results and Discussion

As a contrast to the conventional technique of bath perfusion for drug application to brain slices, our first set of experiments examined the ability of the MFP to selectively administer different concentrations of the AMPA receptor antagonist CNQX to specific cell layers in hippocampus. The hippocampus can be divided into five major, distinct layers in the CA1 region: alveus, stratum oriens, stratum pyramidale, stratum radiatum, and stratum lacunosum-moleculare. In electrophysiological experiments, independent activation of axons in stratum oriens and stratum radiatum is often used as a technique to trigger a pair of spatially separated synaptic inputs to the pyramidal cell population. Two stimulating electrodes (S_1 and S_2) were here placed in stratum oriens and stratum radiatum, respectively, providing activation of Schaffer collaterals, *i.e.*, axon collaterals projecting from CA3 region to CA1, which form synapses with both basal dendrites in stratum oriens and apical dendrites in stratum radiatum of the pyramidal cells in the CA1 region. A recording pipette was inserted into stratum radiatum (Figure 1A), at a distance of 200-500 μm from S_1, for recording of field potentials (fEPSPs). Due to the highly organized and layered structure of the pyramidal cells, synaptic activities at basal dendrites in stratum oriens can be recorded from corresponding apical dendrites in stratum radiatum as reversed fEPSPs (RfEPSPs; see Figure 1A), making it possible to assess synaptic activity of the two synaptic regions via a single recording pipette. This is the basis for our first selectivity test, in which electric activities of the two synaptic layers were compared while the MFP was maintained at a fixed location (see results described below, and Figure 2). In a second type of selectivity test, the MFP delivered CNQX sequentially at different distance points extending horizontally from the tip of the recording pipette (Figure 1B). At each point, CNQX was first delivered with the HCF kept on, recirculating the solution via the aspiration ports of the MFP. After reaching the maximum blocking effect, the aspiration was turned off to measure the effect without recirculation. Before administering CNQX with the MFP at each selected distance, the fEPSP was fully recovered from the previous experiment (see results described below and Figure 3).

As shown in Figure 2A, different concentrations of CNQX were delivered via bath perfusion, which non-selectively reduced the fEPSP and RfEPSP. In contrast to the proportional blockade of potentials by bath application of CNQX, the fEPSP generated in stratum radiatum stimulated by S_1 was selectively reduced by CNQX, delivered via the MFP positioned in the same layer, without affecting the RfEPSP generated in stratum oriens, stimulated by S_2 (Figure 2B). The MFP is thus able to deliver the drug selectively to the apical dendrites of the pyramidal cells, while not affecting the basal dendrites of these cells in the CA1 region of hippocampus. In addition to alternating stimulation by S_1 and S_2, these two electrodes could stimulate oriens and radiatum synapses simultaneously (S_{1+2}), resulting in competitive synaptic activities (hereafter referred to as competitive fEPSP, CfEPSP). For independent synaptic inputs, as those of stratum oriens and stratum radiatum in the present study, the CfEPSP will match the sum of fEPSP and RfEPSP, especially when there is little contamination of fEPSPs by cell firing. As seen in Figure 2A, the CfEPSP was close to zero for all concentrations used, thus providing additional evidence that the two groups of synapses are uniformly affected by bath application of CNQX. On the contrary,

CNQX administered by the MFP to stratum radiatum generated the same “algebraic effect” on the CfEPSP and fEPSP, even though the absolute sizes of these potentials increased and decreased, respectively, upon CNQX application (Figure 2B). These experiments demonstrate that the MFP has the capability of delivering biologically active substances or drugs to defined regions, e.g. cellular layers in a brain slice, without spilling over to other areas. It can conveniently be applied to different areas in the brain slice, providing for easy integration with various monitoring and probing techniques.

In the following set of experiments, we compared the performance of the MFP with and without activated HCF (Figure 3). With the recirculation active, we expected greater distance dependence of the drug effect than in the injection-only mode of operation, *i.e.*, the confined open volume should allow for finer spatial control when delivering biologically active substances to a brain slice. Each measuring point in Figure 3 is the blocking efficiency of CNQX on the AMPA receptor-mediated fEPSP in stratum radiatum, plotted vs. the distance from the point of recording. As illustrated, the CNQX-loaded MFP with deactivated HCF produced an about 60% decrease of the fEPSPs at a distance of 400 μm, whereas in the presence of HCF, there was no blocking effect at this distance. Fitting the data with a pair of Gaussian curves allowed quantification of the spatial profile using the “SD parameter”, roughly corresponding to the width of the curve at a level of 60%. Note, however, that SD is not the standard deviation in this context but a mathematically analogous curve parameter (see caption of Figure 3). The profile widths obtained with and without HCF were 141 ± 13 μM and 357 ± 21 μM ($p<0.001$, $n=5$), respectively. These experiments demonstrate that the effect of CNQX delivered by the MFP occurs more localized in the brain slice in comparison with injection-only delivery, with a more than 2-fold sharpening of the spatial profile.

In a different set of experiments we investigated the ability to switch between multiple different solutions, stored in device-integrated solution reservoirs. This feature of the microfluidic device allows not only to sequentially expose the selected region to a series of active compounds, it also means reduced reagent consumption compared to conventional perfusion systems. The reservoirs can be preloaded with 35 μl of different drugs, or different drug concentrations, the latter allowing for facile and rapid determination of concentration-response profiles. Here we have extended a previous study (see Ahemaiti et al., 2013) by comparing concentration response curves generated by conventional bath perfusion, and by using the MFP (Figure 4A). Four concentrations of CNQX were administered via the MFP. Each concentration was applied until a steady state was reached, *i.e.*, a solution was switched to another containing a higher concentration of CNQX when the previous one had resulted in a maximum effect on the fEPSP. The IC_{50} values of fEPSP inhibition by CNQX delivered with bath perfusion and MFP were determined after fitting the data with sigmoid curves, yielding values of 0.49 μM and 0.87 μM ($p<0.001$), respectively, implying a ratio of 56% (see caption of Figure 4 for details). These results demonstrate that the efficiency of the drug delivery by the MFP is just slightly lower than with bath perfusion. However, compared to bath perfusion, a ∼100 times lower volume of the drug solutions is required.

To explore the small difference in effiency of the MFP as compared to bath perfusion, we simulated the diffusion of CNQX in a mathematical model (Figure 4B, C). The spatial

concentration profile experimentally determined in Figure 3 was here used as input concentration applied to the surface of the slice. Concentration at the bottom of the slice was set to zero as our slice chamber provided double-sided perfusion. In a steady state model, such as the one used here, the exact value of the diffusion constant does not matter, implying that the obtained results are valid for any diffusable substance, including of course CNQX. The simulated spread of the drug by diffusion in the slice, depth-wise and side-wise, is illustrated in Figure 4B. The diagram in Figure 4C, illustrates the calculated change of concentration along a center line from the top to the bottom of the slice. It is seen that at the estimated depth of the recording electrode, ca 100 μm, the drug concentration is about 46% of that applied via MFP, to be compared with the 56% obtained experimentally (see above and Figure 4A).

With respect to a comparison between mass transport using MFP versus bath perfusion, the following remarks can be made. It can be noted that flow velocities have similar values (0.1-1.0 mm/s) for the “concentration blob region” just outside the MFP and for the “main bathing solution” surrounding the slice, which is actively pumped through the tissue chamber. The faster reaction to MFP compared to whole slice perfusion is therefore not because of differences in perfusion/transport speed but due to the time it takes to replace the solution in the chamber. Most of the transport outside the slice is via convection (perfusion) whereas diffusion dominates within the slice. This is due to the fact that hydrostatic pressures are extremely small between regions of the slice. Note that the chamber is fully open upwards and the MFP does not touch the slice, even though one of the edges gets close (see Methods).

Conclusions

Using a recently developed MFP, we here demonstrate high spatial resolution for delivery of drugs or drug candidates at different concentrations to brain slices. Especially, the MFP was able to selectively deliver drugs to different layers of the CA1 region in the hippocampus, and the degree of selectivity was found to be critically related to HCF, which is a key feature of the device. Using the present MFP it will thus be possible to study selected regions of brain slices, integrated with various imaging and probing techniques, without affecting the other parts of the slices.

In this study we have not taken the temporal aspects of superfusion experiments into consideration. We have shown in the previous study that a 60% reduction of the superfusion time is possible compared to bath perfusion. Further systematic studies are under way. They also involve a variety of other active compounds, and technical improvements on the device itself. For example, changes in material and fabrication procedures will allow for a smaller tip size, which will optimize the spatial profile of the confined volume, and further improve its performances in brain slice superfusion.

Acknowledgments

We acknowledge the European Research Council, the Swedish Research Council (VR), the Royal Society of Arts and Sciences in Gothenburg (KVVS), the Wallenberg Foundation, the Åhlén Foundation, the foundations of Gun &

Bertil Stohne and Wilhelm & Martina Lundgren, and the National Institutes of Health (NIH) through grant GM R01-066018.

References

Ahemaiti A, Ainla A, Jeffries GD, Wigstrom H, Orwar O, Jesorka A, Jardemark K. A multifunctional pipette for localized drug administration to brain slices. J Neurosci Methods. 2013; 219:292–296. [PubMed: 23969260]

Ainla A, Jansson ET, Stepanyants N, Orwar O, Jesorka A. A microfluidic pipette for single-cell pharmacology. Analytical chemistry. 2010; 82:4529–4536. [PubMed: 20443547]

Ainla A, Jeffries GD, Brune R, Orwar O, Jesorka A. A multifunctional pipette. Lab on a chip. 2012a; 12:1255–1261. [PubMed: 22252460]

Ainla A, Xu S, Sanchez N, Jeffries GD, Jesorka A. Single-cell electroporation using a multifunctional pipette. Lab on a chip. 2012b; 12:4605–4609. [PubMed: 22810424]

Blake AJ, Pearce TM, Rao NS, Johnson SM, Williams JC. Multilayer PDMS microfluidic chamber for controlling brain slice microenvironment. Lab on a chip. 2007; 7:842–849. [PubMed: 17594002]

Eichenbaum H. The hippocampus and mechanisms of declarative memory. Behavioural brain research. 1999; 103:123–133. [PubMed: 10513581]

Huang Y, Williams JC, Johnson SM. Brain slice on a chip: opportunities and challenges of applying microfluidic technology to intact tissues. Lab on a chip. 2012; 12:2103–2117. [PubMed: 22534786]

Ling G, Gerard RW. The normal membrane potential of frog sartorius fibers. Journal of cellular physiology. 1949; 34:383–396. [PubMed: 15410483]

Neher E, Sakmann B. Single-channel currents recorded from membrane of denervated frog muscle fibres. Nature. 1976; 260:799–802. [PubMed: 1083489]

Rolls ET. A computational theory of episodic memory formation in the hippocampus. Behavioural brain research. 2010; 215:180–196. [PubMed: 20307583]

Stockmeier CA, Mahajan GJ, Konick LC, Overholser JC, Jurjus GJ, Meltzer HY, Uylings HB, Friedman L, Rajkowska G. Cellular changes in the postmortem hippocampus in major depression. Biological psychiatry. 2004; 56:640–650. [PubMed: 15522247]

Tanti A, Belzung C. Neurogenesis along the septo-temporal axis of the hippocampus: are depression and the action of antidepressants region-specific? Neuroscience. 2013; 252:234–252. [PubMed: 23973415]

Travis SG, Huang Y, Fujiwara E, Radomski A, Olsen F, Carter R, Seres P, Malykhin NV. High field structural MRI reveals specific episodic memory correlates in the subfields of the hippocampus. Neuropsychologia. 2014; 53:233–245. [PubMed: 24296251]

Tulving E, Markowitsch HJ. Episodic and declarative memory: role of the hippocampus. Hippocampus. 1998; 8:198–204. [PubMed: 9662134]

Highlights

- A microfluidic device for localized drug perfusion to brain slices is presented.
- The device performance is characterized.
- The tool utilized hydrodynamically confined flow for localized drug delivery.
- The drug delivery efficiency of the tool is comparable with whole slice perfusion.
- The tool requires orders of magnitude less drugs than whole slice perfusion.
- The tool can be used in combination with other probing and imaging techniques.

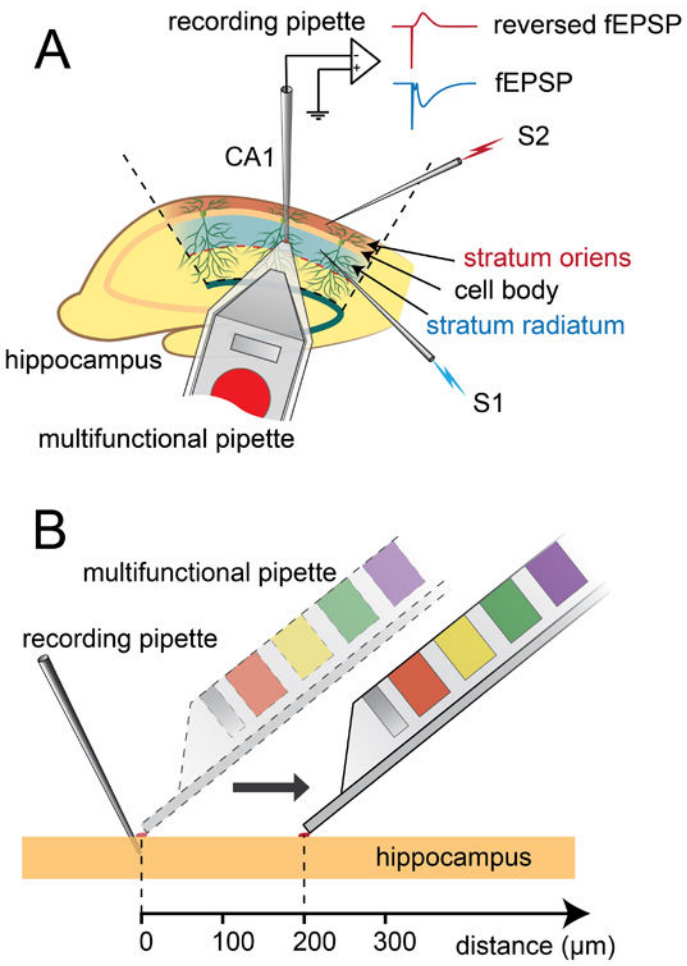

Figure 1.

Figure A shows the basic experimental setup configuration. Stimulating electrode 1 (S_1) is inserted in stratum radiatum and stimulating electrode 2 (S_2) is inserted in stratum oriens. A recording pipette is placed in stratum radiatum and different concentrations of the AMPA receptor antagonist CNQX are applied to the tissue surface via the multifunctional pipette (MFP). The field potential (fEPSP) in stratum radiatum induced by S_1 is directly recorded by the recording pipette and the field potential in stratum oriens induced by S_2 is also recorded by the (same) recording pipette but in reversed form (reversed fEPSP). Figure B demonstrates the application of CNQX with MFP at different distances from the recording pipette.

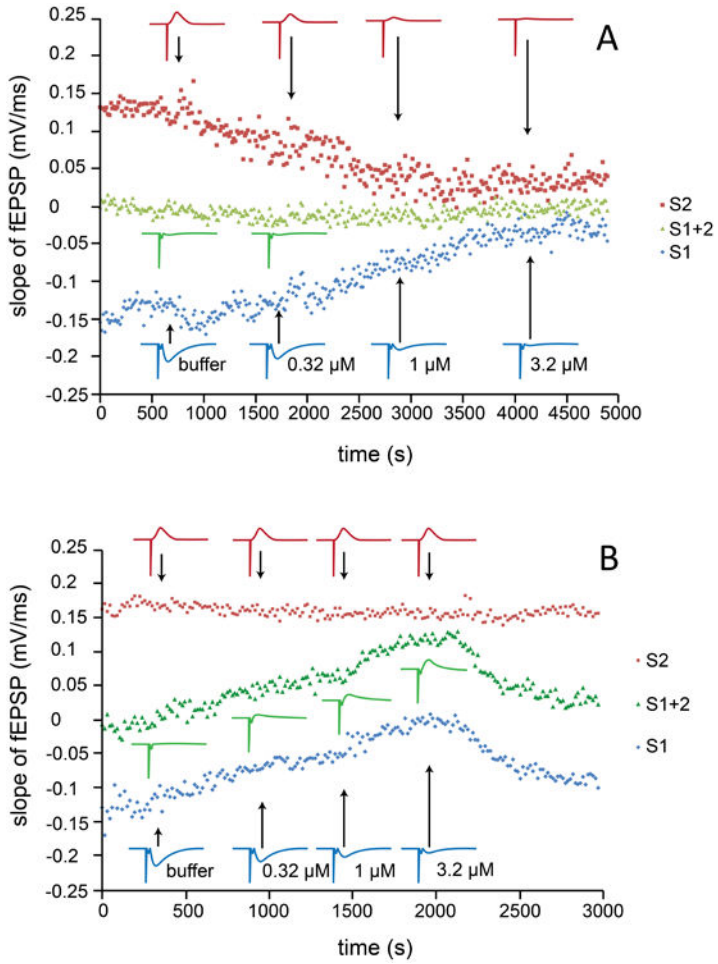

Figure 2.

Each data point represents the slope value of fEPSPs recorded at stratum radiatum. Stimulating pulse 1 (S_1) was given at stratum radiatum, S_2 was given at stratum oriens, for which the corresponding reversed fEPSP values were recorded with the same recording pipette placed in stratum radiatum (compare Fig. 1A). S_{1+2} was third stimulation mode, where S_1 and S_2 were given simultaneously. The stimulus protocol S_1, S_2, S_{1+2} was continuously repeated throughout the experiment. Different concentrations of CNQX were delivered via bath perfusion and field potentials from stratum radiatum and stratum oriens were found to be reduced in parallel (panel A, representative data from a total of 7 experiments), whereas administration via MFP selectively blocked the fEPSP in one layer without affecting another (panel B, representative data from a total of 5 experiments). The results are consistent with the effect/noneffect of CNQX on the competitive fEPSP induced by simultaneous S_1 and S_2 (see text for further explanation). Insets show traces for fEPSPs obtained by S_1 or S_2 stimulation.

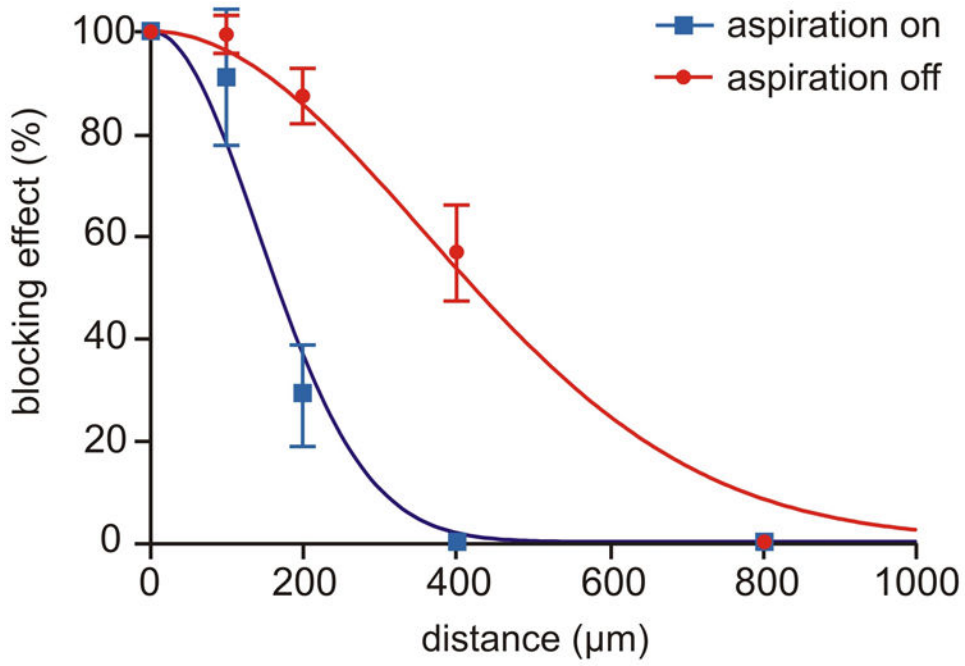

Figure 3.

Spatial drug delivery profile of the MFP, with and without the feature of hydrodynamically confined fluid (HCF). CNQX (5 μM) was applied via the MFP to brain slices at different distances from the recording site, using 100 μm steps (compare Fig. 1B). The MFP was alternated between two modes: with (suction on, blue curve) and without (suction off, red curve) hydrodynamically confined microflow. Data are shown as mean ± S.E.M for 5 experiments, each of which provided both “on” and “off” measurements. The fitted Gaussian curves, as defined by $y=100\ \exp(-(x/SD)^2/2)$, illustrate that HCF leads to a more narrow drug delivery profile, curve-SD being 141 *vs.* 357 μM, $p<0.001$.

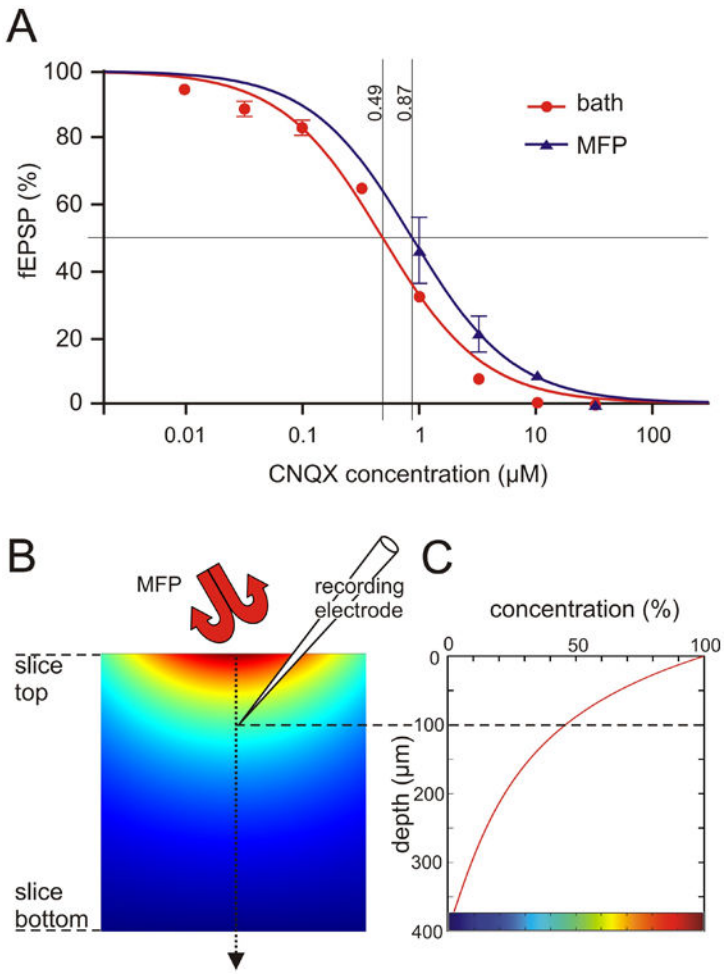

Figure 4.

Concentration response curves for bath perfusion and MFP (A) and comparison with a diffusion model (B, C). In Figure A, each data point was the percentage of fEPSP slope after application of a certain concentration of CNQX compared with the value under drug-free buffer, testing concentrations from 10 nM to about 30 μM in equal logarithmic steps (data from 8 bath and 4 MFP experiments, shown as mean ± S.E.M.). Curve fitting used a reverse Hill equation with slope constrained to 1, y=100/(1+(c/IC50)), appearing sigmoid when plotted semilogarithmically as a function of $\log_{10}(c)$. It can be seen that the drug delivery efficiency of the MFP was slightly smaller than that of bath perfusion, with corresponding IC50 values of 0.49 μM and 0.87 μM ($p<0.01$), implying a relative efficiency of 56%. B. Cross section of brain slice diffusion model with a Gaussian-shaped concentration profile on top, using the fitted “HCF on curve” in Figure 3 as template, and surrounded elsewhere by zero concentration. The simulated steady state concentration of CNQX is visualized by pseudocolors. C. Plotting the calculated concentration along the center line, from top to bottom of the slice, reveals that at an estimated recording depth of 100 um, the drug concentration is about 46% of the one applied. Colorbar at bottom of C refers to pseudocolors in B.